Research on Microscopic Characteristics of Interfacial Transition Zone of Recycled Coarse Aggregate Asphalt Mixture

Changjiang Kou [1, 2] *, Mengyun Zhang [1], Aihong Kang [1, 2], Peng Xiao [1, 2], Haotian Hu [3]

[1] College of Civil Science and Engineering, Yangzhou University, Yangzhou 225127, China;

[2] Academy of Urban Planning and Development, Yangzhou University, Yangzhou 225127, China;

[3] Jiangsu Sutong Bridge Co., Ltd, Nantong 226000, Jiangsu, China.

Corresponding author: Changjiang Kou, changjiang.kou@yzu.edu.cn, 15861320609.

Highlights

Identification of interfacial transition zones in RCAM

Formation of NI, SEM microscopic inspection methods and standardised specimen preparation methods for asphalt mixtures

Analysis of the mechanical parameters, micromorphological characteristics and elemental composition of the interface transition zones in RCAM

Abstract

In order to quantitatively characterize the mortar-natural aggregate interface transition zone (M-N ITZ) and mortar-asphalt mastic interface transition zone (M-A ITZ) in the recycled coarse aggregate asphalt mixture (RCAM), and to obtain the microscopic characteristics, chemical characteristics and structural composition of the ITZs, the nano-indentation (NI) and scanning electron microscopy (SEM) were used to test and analyze the nano-mechanical parameters, microscopic characteristics and chemical elemental composition of the ITZs. The results show that in terms of nanomechanical parameters, M-N ITZ is uniformly distributed on the surface of the natural aggregate with a thickness of 25 μm and an average modulus of elasticity of 24.01 GPa, while the M-A ITZ has a thickness of 26 μm and an average modulus of elasticity of 28.68 GPa. In terms of microscopic morphology, the mastic near the surface of the aggregate in M-A ITZ is denser than the distant mastic. M-N ITZ has good integrity between the phases, but as the aggregate moves away from the phase interface, the agglomeration effect diminishes resulting in uncompacted pores within.

Keywords: recycled coarse aggregate asphalt mixture (RCAM); micro-nano characteristics; interfacial transition zone (ITZ)

1. Introduction

As China's urbanisation process continues, the increasing shortage of natural gravel resources and the increasing accumulation of construction and demolition waste (C&DW) will gradually become one of the main contradictions in China's construction engineering sector. Waste concrete is a major component of C&DW [1-2]. Recycled coarse aggregates (RCAs) obtained by processing and crushing waste concrete are proven to be used in the preparation of RCA asphalt mixture (RCAM), which can be used to pave asphalt pavements of different grades. Asphalt mixtures with RCAs replacing natural aggregates have shown good performance [3-4]. It can promote the efficient use of construction waste and reduce the consumption and extraction of natural sand and gravel. Therefore, with the development of road construction, the use of RCAs for asphalt pavements is a highly promising issue.

The feasibility of using RCA in asphalt mixtures has received increasing attention from researchers. Different from natural aggregates, RCAs are composite materials that have minor damages and porous cement mortar attached to the surface [5-6]. Pedro et al. [7-8] found that compared to natural aggregates, RCAs have high water absorption, low specific gravity, high abrasion and high pressure crushing values, but meet some of the engineering requirements. Poon et al. [9-11] found that the adhering mortar layer leads to a rough, heterogeneous and porous surface of the RCAs, resulting in increased micro-damage and deterioration of the physical and mechanical properties of RCAM. So moisture can easily intrude and remain in the highly developed pores of the cement mortar in RCA [12]. As a result, the adhesion between RCA and asphalt is more severely degraded than with natural aggregates. Wu et al [13-15] earlier demonstrated the feasibility of recycled aggregates applied to asphalt mixes. The higher the RCA content, the higher the asphalt absorption and stability of the RCAM [16]. Mills-Beals et al [17-19] incorporated partially recycled aggregates into asphalt mixes and the freeze-thaw splitting tensile strength ratio, modulus of elasticity and dynamic modulus of the asphalt mixes decreased as the number of recycled aggregates was increased. However, Pérez et al [20] suggest that limiting RCA to an appropriate content can ensure that the asphalt mix meets the performance requirements for water stability. In addition, numerous studies have shown that the use of RCA increases the low-temperature cracking tendency of asphalt mixtures. Bhusal et al [21] found that the indirect tensile strength of asphalt mixes containing RCA was lower than that of asphalt mixes containing natural aggregates. On the other hand, Shen et al [22-23] indicated that coarse RCA could improve the high-temperature rutting resistance of asphalt mixtures. Meijide et al [24-25] found that although recycled aggregates reduced the spalling resistance of asphalt stabilised materials, they substantially increased the resistance to permanent deformation. In summary, the performance of asphalt mixtures containing RCA over their service life is very different from that of conventional mixtures.

The performance of recycled aggregate asphalt mixes is directly related to the bond strength at the interface between the materials. Zhu et al [26] found by SEM that the cementitious material formed a narrow region around the aggregate particles, which was considered to be the interface transition zone (ITZ). The interaction mechanism at the asphalt-aggregate interface is critical. Matzenmiller et al [27-28] also found that the interfacial bond strength has an effect on the overall performance of the composite and that identifying the interface between the asphalt and the aggregate surface connection helps to control the mechanisms of fracture behaviour in asphalt pavements. The mechanical properties of ITZs are extremely complex, so ITZs become the weak point of RCAM [26,29]. Hu et al. [30] divided the interfacial zone in the RCAM into the cement mortar interface and the natural aggregate interface. Increasing the RA percentage leads to more interfacial damage, with interfacial damage at the cement mortar and asphalt mortar being the main source of damage. It is therefore valuable to study the nature of the transition zone at the interface of recycled aggregate asphalt mixes. However, the lack of understanding of the microscopic properties of the transition zone at the RCA - asphalt mortar interface now directly affects the study of the mechanical properties and damage patterns of RCAM.

The microstructure of the interfacial transition zone in asphalt mixtures can be explored by several instrumental techniques (scanning electron microscopy (SEM), nanoindentation, atomic force microscopy, X-ray, etc.) to help understand the complex mechanical behaviour of the interfacial transition zone of recycled aggregate asphalt mixtures [31-33]. Anna et al. [34-35] studied the interface between the aggregate and cement paste by SEM. Barbhuiya et al. [36] investigated the nanomechanical properties of asphalt mixes in the mastic, ITZ and granite aggregate phases. Hu et al. [37] further measured the mechanical behaviour of the interface zone by nanoindentation and found that the influence of aggregate type on the ITZ range was evident, with limestone producing a smaller range of ITZ compared to basalt and gabbro. Similarly, Huang et al. [12] found through NI tests that the thickness of ITZ in asphalt mixes with more porous cement mortars and bricks (40μm) was thicker than that of dense recycled granite and natural limestone (30μm). It has also been shown that the ITZ ranges from 30 to 60μm near the surface of the aggregate [38]. Khorasani et al [39] concluded that the hardness and modulus values of the ITZ are between those of limestone aggregates and asphalt marl. Lee et al [40-41] found that the thicknesses of the old and new interfacial transition zones were about 40-50 μm and 55-65 μm, respectively, at late stages, while the average moduli of the new and old interfacial transition zones were about 70-80% of that of the old slurry matrix and 80-90% of that of the new slurry matrix, respectively. Li et al [42] investigated the distribution of chemical elements in the focal region using energy dispersive spectroscopy (EDS) combined with SEM imaging to obtain more accurate thicknesses and to identify each phase of the asphalt mixture by analysing the characteristic elements. However, current research is still very limited in understanding the microscopic mechanical properties of the nanoscale interfacial transition zone in recycled aggregate asphalt mixtures.

Therefore, this study intends to complete the design of the RCAM, and use advanced microscopic testing methods to examine the micromechanics, apparent morphology, and elements of the transition zone of the RCA-asphalt mastic interface.

2. Materials and mixtures design

2.1 Materials

The aggregates used in this experiment include crushed production of RCAs and natural aggregates. Among them, RCAs are all derived from waste cement concrete panels. RCAs in different particle size ranges are shown in **Fig.1**. The particle size range of the recycled aggregates used in this study is 9.5-26.5mm. The general properties of RCA and natural aggregate meet the application Criteria of asphalt mixture coarse aggregate.

(a)26.5-31.5mm (b) 9.5-26.5mm (c) 0.75-9.5mm

Fig. 1. RCAs in different particle size ranges

Compared to natural aggregate, RCA of various particle sizes has the characteristics of reduced density, increased water absorption, large crushing value, and large loss of Los Angeles abrasion. Compared to natural coarse aggregates, RCA has a crushing value of up to 23% and a Los Angeles abrasion loss of up to 23.98%, but still meets the requirements of China's technical specifications for the construction of highway asphalt pavement (JTG F40-2004) [43].

To keep RCAM from cracking, rutting, and moisture damage, the asphalt binder used should have a high viscosity and good adhesion with aggregate. The asphalt binder selected was styrene butadiene styrene (SBS) modified asphalt**.** The limestone powder produced by Zhenjiang Gaozi is selected as the ore powder.

2.2 Mixture design

In this study, RCAs ranging from 9.5 to 26.5 mm were selected to replace natural aggregates of the corresponding particle size according to the AC-20 gradation. The total replacement rate was 39%. Considering the characteristics of the RCA such as the relative density of the gross volume becomes smaller and the cement mortar adhering to the surface, the AC-20 mineral gradation of the RCA mix is adjusted by using the volume correction of the RCA replacement rate and combining with the natural fine aggregate curve fitting method. The gradation curve is illustrated in **Fig. 2**. Using the standard Marshall test method, it is determined that the best oil-stone ratio of natural aggregate AC-20 is 4.4%, the best oil-stone ratio of RCA AC-20 is 4.9%, and the best oil-stone ratio of natural aggregate SMA-13 is 6.0 %, the best oil-stone ratio of RCA SMA-13 is 6.6%. Then Superpave gyratory compactor was employed to compact the asphalt mixture into cylindrical specimens measuring 150 mm in diameter and 115 mm in height.

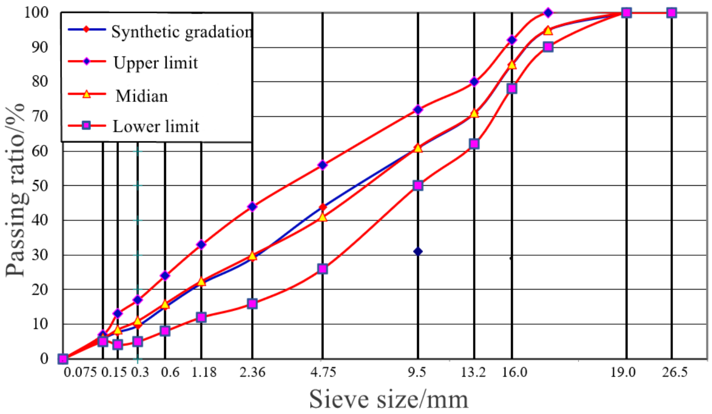

Fig. 2. Gradation curve of asphalt mixture AC20 used in this study

3. Methods

3.1 Nanoindentation test

3.1.1 Nanoindentation test sample preparation

NI test accuracy has a high correlation with the flatness of the specimen surface [44]. Therefore, it is important to try to eliminate the negative effects of uneven surfaces on test results during sample preparation.

The preparation process of a test sample is shown in **Fig. 3.** In order to ensure the surface quality after polishing and grinding, the polished samples were further evaluated by a 3D confocal laser microscope to obtain the surface morphology information. The root mean square (RMS) of the surface morphology was selected to measure the surface roughness. The test result shows that the average RMS roughness of asphalt mastics after polishing is 127.03 nm, which meets the flatness requirements of the scored specimen.

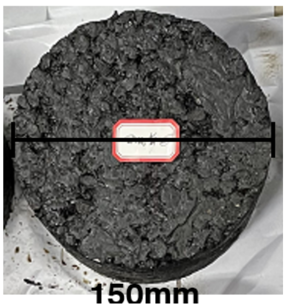

(a) SGC specimen

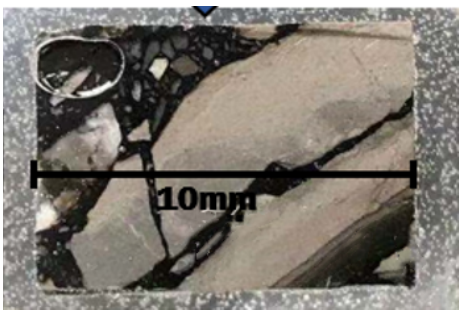

(b) Curing of the small piece cut from the SGC specimen

(c) Vacuum defoaming

(d) Grinding and polishing

(e) Ultrasonic cleaning

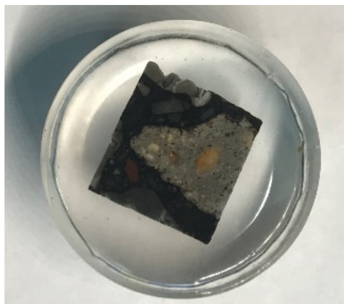

(f) NI test sample

Fig. 3 Sample preparation for NI test

3.1.2 Elastic modulus

Nanoindentation, as a new type of micro-mechanical performance testing technology suiTable for multi-phase mixtures, can identify and characterize multiple phases of asphalt mixtures and characterize the changes in mechanical properties of the transition zone between the new and old interfaces [12]. As shown in **Fig. 4**, this study used Hysitron Triboindenter (TI950) to test the test piece, to determine the nanomechanical properties of the ITZ. The test process is shown in **Fig. 5**.

A grid nanoindentation test was performed on each sample using a nanoindenter (Micro Materials) equipped with a Berkovich tip. The test temperature was set at 25°C. The indentation depth was controlled to within 10,000 nm. The maximum load per phase of the asphalt mix was selected as 3000 μN. The single loading time was set to within 20 seconds [45-46]. The unloading rate is the same as the loading rate. The distance between adjacent points was set to 10 μm. The distance between two test points on the longitudinal line was set to 10 μm. The area covering the aggregate, the ITZ and the asphalt mastic was selected by optical microscopy as the indentation location for the test.

Fig. 4 Nanoindentation instrument HT (TI950)

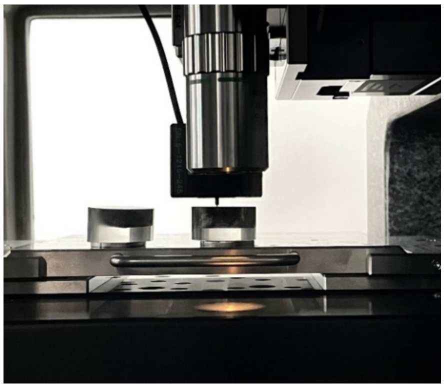

Fig. 5 Indentation testing of samples

3.2 Electron microscope observation

In this study, field emission scanning electron microscopy (FESEM) and environmental scanning electron microscopy (ESEM) [47-48] were used in order to achieve microscopic morphological characterisation of bitumen binders and mixtures to obtain detailed individual phase imaging as well as microstructure. All analyses were carried out at a beam acceleration of 15 KV, with the beam incident perpendicular to the surface and working at a distance of 8 mm. Since vacuum treatment is required to carry out the scanning tests, and as asphalt mixtures are porous materials not easily achievable, the samples needed to be prepared for the test requirements.

As with the NI test sample preparation process, small pieces of epoxy-coated recycled aggregate asphalt mixtures were made. After curing, a precision cutter was used to cut specimens of approximately 10*10*5 mm in length, width and height. The cut specimen contains a uniform and flat test area of recycled aggregate - residual mortar - asphalt mastic. The sample preparation process for SEM test is shown in **Fig. 6**.

(a) Cured RCAM (b) Precision cutting (c) SEM test samples

Fig. 6. Sample preparation for SEM test

4 Results and discussion

4.1 Micromechanical properties of ITZs in RCAM

4.1.1 Elastic-mechanical characteristics of RCAM

The joint interface of the RCA asphalt mix is composed of five different phases, in order of extension from the aggregate: aggregate, M-N ITZ, mortar layer, M-A ITZ, and asphalt. Due to the heterogeneity of the interfacial transition zone, single-phase testing was required to identify the phase composition by selecting the corresponding areas from different samples. Indentation tests on a 10*10 grid were carried out on each phase. The loading-unloading curves of each indentation were recorded, and the modulus of single material in **Tab. 5** was obtained from the elastic unloading curve by using the Oliver-Pharr method.

Tab. 5 Average modulus and coefficient of variation of different materials

Material	Cement mortar	Modified asphalt	Aggregate
Modulus /GPa	30.23	1.62	50.65
Coefficient of Variation /%	31.2	15.8	12.5

In addition to representing the mechanical properties of the different phases, the grid indentation technique also allows the characteristics of the indentation curve for each phase, as shown in **Fig. 7**. Different phases exhibit different maximum indentation depths for the same indenter with constant loading and unloading speed and maximum control load. The maximum indentation depth allows clear identification of the different phases and facilitates the identification of multi-phase interface indentations. The bituminous phase can reach an indentation depth of over 2000nm with an average modulus of 1.62GPa; the natural aggregate has good mechanical properties with an indentation depth of 800-1000nm and an average modulus of 50.65GPa for the same test method; the cement mortar layer has an indentation depth between 1000-1500nm and shows a similar loading-depth diagram as the natural aggregate, but As can be seen from the loading and modulus distinctions, the load-depth curves characterise the asphalt, natural aggregate and cement mortar well and can distinguish between the different zones well.

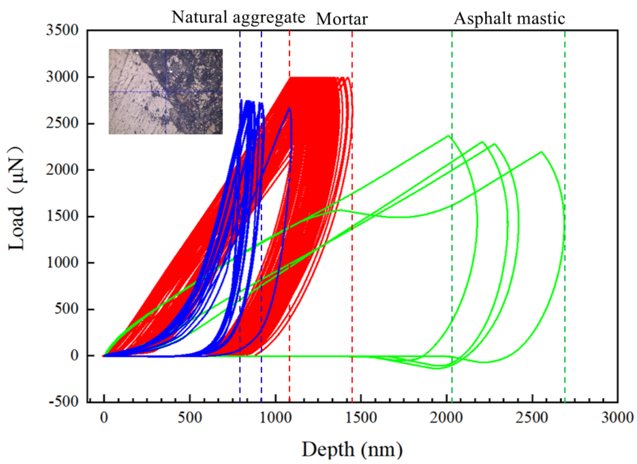

Fig. 7 Indentation curves for aggregates, mortars and asphalt mastics

4.1.2 Elastic-mechanical characteristics of M-A ITZ

In this study, a suiTable test area in **Fig. 8** was selected and indentation tests were carried out on M-A ITZ. The load-displacement curve obtained is shown in **Fig. 9**. The results show that the indentation modulus in the area of the old slurry matrix adjacent to the new interfacial transition zone is significantly higher than in the asphalt area. Using the modulus data obtained from the NI tests, indentation modulus contour maps were drawn for the area of the M-A ITZ and used to examine the mechanical properties independently of each other, as shown in **Fig. 10**. The modulus contour maps were not uniformly distributed due to the asphalt mastic and weak mortar, and large deviations occurred in the longitudinal and lateral averaging statistics. In this study, frequency statistics were determined concerning the modulus contour images for suiTable intervals and the statistical averages and deviations were applied to the modulus histograms over M-A ITZ. The modulus frequency diagram over M-A ITZ is shown in **Fig. 11**, which allows the indentation modulus distribution in specific directions to be identified and the thickness of M-A ITZ to be determined. By analysing the lateral variation of properties around the aggregate, the thickness of the transition zone at the new interface is 26 μm. The results show that the average modulus of the transition zone at the new interface is 28.68 GPa.

The modulus frequency diagram represents the trend in the modulus of elasticity from the asphalt mastic phase to the aggregated phase. Between 0 and 40 μm on the grid distance, the material is in the asphalt mastic phase, where the modulus is at a low level of approximately 0-5 GPa. The small amount of fine mineral fines contained in the mastic phase causes the modulus to fluctuate. Between 40 and 66 μm on the grid distance, in M-A ITZ, the modulus is between 10 GPa and 25 GPa. Beyond 66 μm, the modulus continues to increase rapidly and more rapidly in the test area near the mortar side.

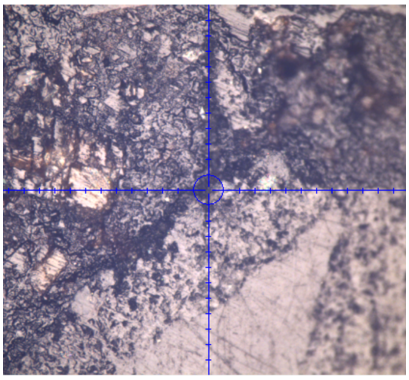

Fig. 8 M-A ITZ test area

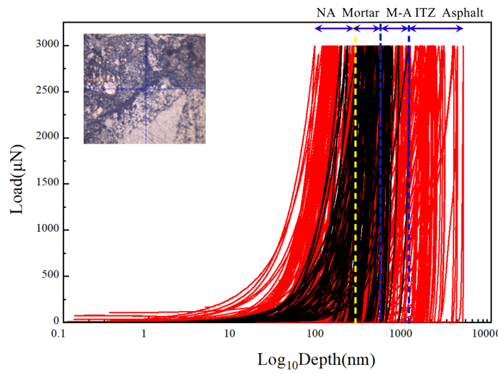

Fig. 9 The load-displacement curve in M-A ITZ

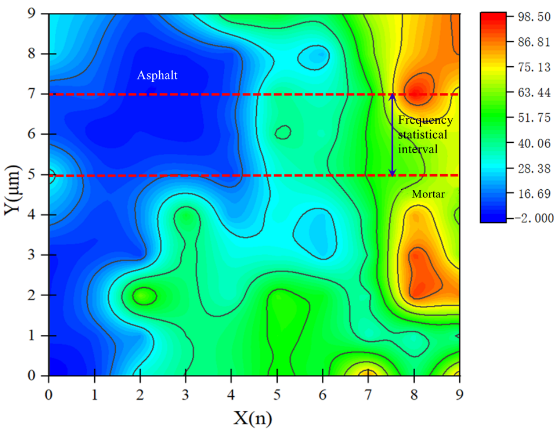

Fig. 10 Modulus contour map of M-A ITZ

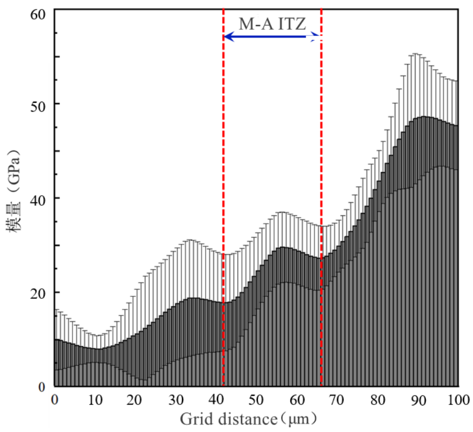

Fig. 11 Modulus frequency diagram of M-A ITZ

4.1.3 Elastic-mechanical characteristics of M-N ITZ

In order to obtain a representative distribution of the mechanical properties in the M-N ITZ, a grid area of 100 indentation points was tested in the M-N ITZ test area in **Fig. 12.** The load-displacement curve obtained is shown in **Fig. 13**. The modulus contour map and modulus frequency diagram of M-N ITZ obtained by the same method as M-A ITZ are shown in **Fig. 14** and **Fig. 15**. By analysing the lateral variation of properties around the aggregate, the M-N ITZ is 25 μm thick. The average modulus of M-N ITZ is 24.01 GPa, which is 1.3-1.5 times the average modulus of cement mortar.

The modulus frequency diagram represents the trend in the modulus of elasticity from the cement mortar phase to the natural aggregate phase. The grid distance is between 0-15 μm, in the mortar phase, when the modulus of the material is at a low level, 0-3 GPa, and the small amount of uncracking contained in the mastic phase causes its average modulus to decrease and is prone to numerical fluctuations. Between 15-40 μm, in the M-N ITZ, the modulus is between 10 GPa and 30 GPa. gradually approaching the aggregate zone, the modulus of elasticity of the material all increases sharply at a 10 μm distance and then the growth rates of both indicators slow down as the distance increases for each sample. Beyond 85μm, the modulus of the material continues to increase gradually, and begins to slow down as it reaches the dense region. This phenomenon of high modulus and stability in the outer layer of the M-N ITZ may be due to the concentration of fine mineral powder and hydrated crystals in the interface region, which is consistent with the conclusions obtained by SEM. From the modulus isogram, it can be observed that the M-N ITZ is mainly distributed along the outer part of the natural aggregate and has a uniform thickness distribution.

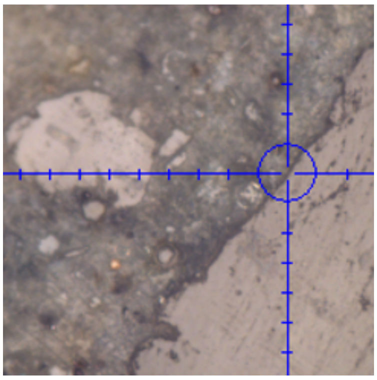

Fig. 12 M-N ITZ test area

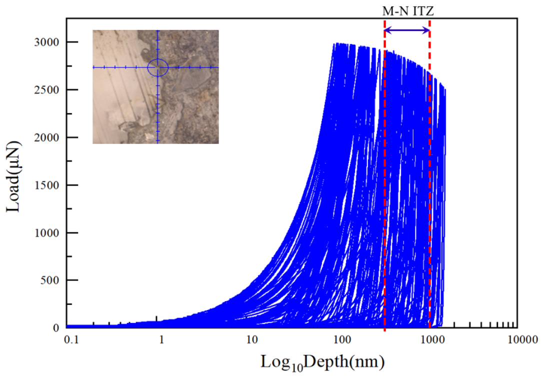

Fig. 13 The load-displacement curve in M-N ITZ

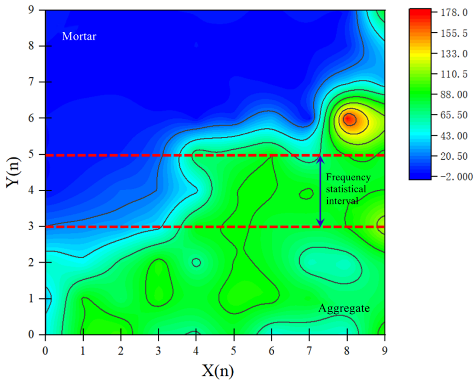

Fig. 14 Modulus contour map of M-N ITZ

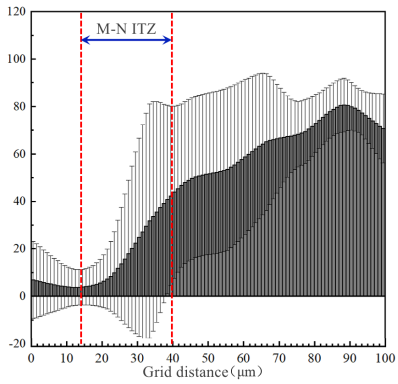

Fig. 15 Modulus frequency diagram of M-N ITZ

4.2 Microstructure of ITZs in RCAM

The existence of a clear boundary between the asphalt mastic and the M-A ITZ was visually verified by SEM images. The ITZ area was identified using the density variation with crystal distribution. The asphalt mastic was applied to the RCA surface. The stronger M-A ITZ is provided by filling the voids and cracks in the old slurry matrix adhering to the RCA. The creation of denser areas of M-A ITZ close to the asphalt can be explained by the chemical adhesion capacity. As the M-A ITZ moves away from the bitumen and closer to the mortar area, less chemisorption occurs due to the weaker connectivity between it and the carbonised calcium oxide on its surface, which leads to a loosening of the structure and pores allowing larger gaps to be created between them. The M-A ITZ, as the location of the asphalt mastic-mortar phase connection, has an internal gap of 2-5 μm, which may be caused by the accumulation of poor particles of mineral dust and fine aggregates, which enter the area near the interface preventing the penetration of the asphalt mastic, as shown in **Fig. 16** and **Fig. 17**.

The main reasons for the production of the M-N ITZ zone are chemical forces as well as hydration reactions. The hydrate in the M-N ITZ zone has some well-crystallised flocculated CH and a moderate amount of whisker-like calcarenite crystals, as well as some free silica. The significantly higher porosity, free silica and CH crystals in the M-N ITZ compared to the aggregate implies that conditions for hydration reactions existed in the M-N ITZ area in the later stages, allowing for higher moduli to be obtained, and the M-N ITZ range can be effectively identified by identifying the characteristic elements silicon (Si) and aluminium (Al) in the hydration products. The M-N ITZ has better adhesion compared to the M-A ITZ. Although gaps exist between M-N ITZ and RCAs, the chemical reaction over a long period of time results in the hydration products gradually sealing the pores, resulting in a better integrity between M-N ITZ and the mortar interface, as shown in **Fig. 18**. However, due to the fact that the interior of the M-N ITZ is far away from the aggregate, a better agglomeration effect has not been produced resulting in an uncompacted hollow inside the M-N ITZ, as shown in **Fig. 19**.

A large number of uncompacted pores and joints between the interfaces cause great harm to the performance of the transition zone between the new and the old interface, which causes stress concentration and damages the firmness of the connection between the aggregate gravel and the asphalt mastic. This may be the transition zone of the connection position. One of the reasons why it is easy to destroy first.

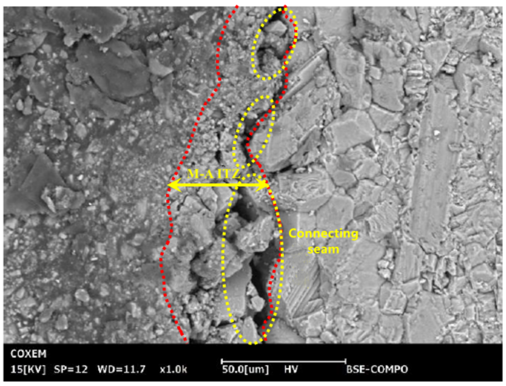

Fig. 16. Joint seams in M-A ITZ

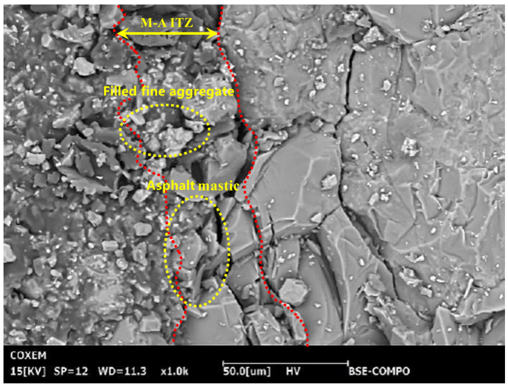

Fig. 17. The internal structure of M-A ITZ

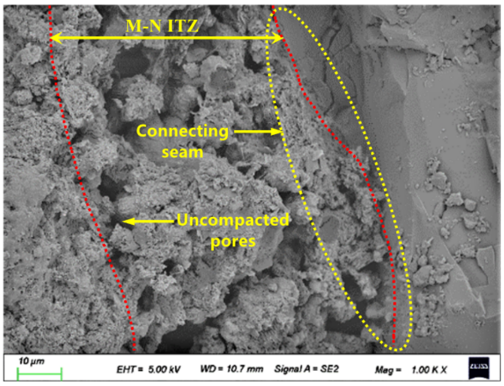

Fig. 18. Chemical composition in M-N ITZ

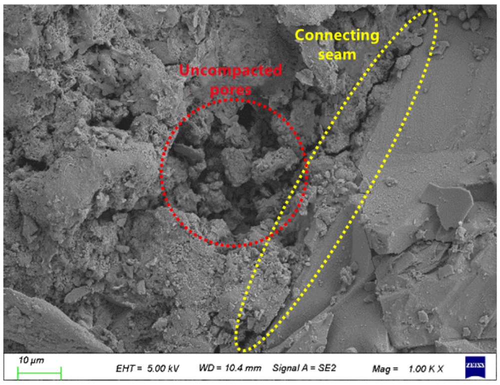

Fig. 19. Connection joints and uncompacted pores in M-N ITZ

5. Conclusion

In order to investigate the microscopic properties of the interfacial transition zone of RCA and asphalt mastic, this study proposes a method for the preparation of microscopic observation samples of the interfacial transition zone on the proportional design of RCAM. The micromechanical parameters of different phases in the interfacial transition zone were investigated using nanoindentation. The microscopic morphological characteristics of the transition zone between the old and new interfaces were investigated using scanning electron microscopy (SEM).

a. Analysis of the modulus contour plot and modulus frequency plot of the ITZ shows that the M-N ITZ is uniformly distributed over the surface of the natural aggregate. The average modulus of elasticity of the M-N ITZ is 24.01 GPa and the thickness is 25 μm. The average modulus of elasticity of the M-A ITZ is 28.68 GPa and the thickness is 26 μm.

b. The structure of the M-A ITZ transitions from a dense area to a loose area. The M-A ITZ is mainly composed of bituminous mastic and fines. The M-N ITZ has good integrity between the interfaces of the phases and is mainly composed of mortar and filler. Some areas of the ITZ are characterised by uncompacted pores and micro-cracks, which can easily cause stress concentration and lead to structural damage.

Acknowledgments

All authors gratefully acknowledge the financial support from National Natural Science Foundation of China (Grant Number 51908487), Natural Science Foundation for Youths of Jiangsu Province (Grant Number BK20190913), Industry-University-Research Collaboration Project of Jiangsu Province (BY2021509), Postgraduate Research & Practice Innovation Program of Jiangsu Province (SJCX21_1582), the Jiangsu Science and Technology Association Promotion Project for the Youths (Grant Number 2021-090) and the Outstanding Young Backbone Teacher of Blue Project of Yangzhou University.

References

[1] Tam, V.W.Y.: Economic comparison of concrete recycling: a case study approach. Resour. Conserv. Recycl. 52 (5), 821-828(2008)

[2] Kim, G.D., Kim, T.B.: Development of recycling technology from waste aggregate and dust from waste concrete. J. Ceram. Process. Res. 8 (1), 82-86(2007)

[3] Sun, D.Q., Tian, Y., Sun, G.Q., Pang, Q., Yu, F., Zhu, X.Y.: Performance evaluation of asphalt mixtures containing recycled concrete aggregates. International Journal of Pavement Engineering. 19 (5), 422-428(2018)

[4] Alvarez, D.A., Aenlle, A.A., Tenza-Abril, A.J., Ivorra, S.: Influence of Partial Coarse Fraction Substitution of Natural Aggregate by Recycled Concrete Aggregate in Hot Asphalt Mixtures. Sustainability. 12 (1), 250(2020)

[5] Paranavithana, S., Mohajerani, A.: Effects of recycled concrete aggregates on properties of asphalt concrete. Resources Conservation and Recycling. 48 (1), 1-12(2006)

[6] Shi, C., Li, Y., Zhang, J.: Effects of recycled concrete aggregates on properties of asphalt concrete. Journal of Cleaner Production. 112, 466-472(2016)

[7] Pedro, D., de Brito, J., Evangelista, L.: Influence of the use of recycled concrete aggregates from different sources on structural concrete. Construction and Building Materials. 71, 141-151(2014)

[8] Poon, C.S., Kou, S.C., Lam, L.: Use of recycled aggregates in molded concrete bricks and blocks. Construction and Building Materials. 16, 281-289(2002)

[9] Poon, C.S., Shui, Z.H., Lam, L.: Effect of microstructure of ITZ on compressive strength of concrete prepared with recycled aggregates. Construction and Building Materials. 18, 461-468(2004)

[10] Ghaffar, S.H., Burman, M., Braimah, N.: Pathways to circular construction: an integrated management of construction and demolition waste for resource recovery. Journal of Cleaner Production. 244, 118-125(2020)

[11] Mercante, I.T., Bovea, M.D., Ibáñez-Forés, V.: Life cycle assessment of construction and demolition waste management systems: a Spanish case study. Int. J. Life Cycle Assess. 17, 232-241(2012)

[12] Huang, Q.B., Qian, Z.D., Hu, J., Zheng, D., Chen, L.L., Zhang, M., Yu, J.Z.: nvestigation on the properties of aggregate-mastic interfacial transition zones (ITZs) in asphalt mixture containing recycled concrete aggregate. Construction and Building Materials. 269, 121257(2021)

[13] Wu, S., Zhong, J., Zhu, J.: Influence of demolition waste used as recycled aggregate on performance of asphalt mixture. Road Materials and Pavement Design. 14 (3), 679-688(2013)

[14] Hou, Y., Ji, X., Su, X.: Laboratory investigations of activated recycled concrete aggregate for asphalt treated base. Construction and Building Materials. 65, 535-542(2014)

[15] Zou, G., Zhang, J., Liu, X.: Design and performance of emulsified asphalt mixtures containing construction and demolition waste. Construction and Building Materials. 239, 117-138(2020)

[16] Espino-Gonzalez, C.U., Martinez-Molina, W., Alonso-Guzman, E.M., Chavez-Garcia, H.L., Arreola-Sanchez, M., Sanchez-Calvillo, A., Navarrete-Seras, M.A., Borrego-Perez, J.A., Mendoza-Sanchez, J.F.: Asphalt Mixes Processed with Recycled Concrete Aggregate (RCA) as Partial Replacement of the Natural Aggregate. Materials. 14 (15), 4196(2021)

[17] Mills-Beale, J.L., You, Z.P.: The mechanical properties of asphalt mixtures with Recycled Concrete Aggregates. Construction and Building Materials. 24, 230-235(2010)

[18] Xiao, F., Yao, S., Wang, J.: A literature review on cold recycling technology of asphalt pavement. Construction and Building Materials. 180, 579-604(2018)

[19] Yan, Y.u., Roque, R., Cocconcelli, C.: Evaluation of cracking performance for polymer-modified asphalt mixtures with high RAP content. Road Mater. Pavement Design. 18, 450-470(2017)

[20] Pérez, I., Pasandín, A.R., Gallego, J.: Stripping in hot mix asphalt produced by aggregates from construction and demolition waste. Waste Manag. Res. 30 (1), 3–11(2012)

[21] Bhusal, S., Li, X., Wen, H.: Evaluation of effects of recycled concrete aggregate on volumetrics of hot-mix asphalt. Transp. Res. Rec. 2205 (1), 36–39(2011)

[22] Shen, D.H., Du, J.C.: Evaluation of building materials recycling on HMA permanent deformation. Constr. Build. Mater. 18 (6), 391–397(2004)

[23] Shen, D.H., Du, J.C.: Application of gray relational analysis to evaluate HMA with reclaimed building materials. J. Mater. Civ. Eng. 17 (4), 400–406(2005)

[24] Meijide, B.G., Perez, I.: Binder-aggregate adhesion and resistance to permanentdeformation of bitumen-emulsion-stabilized materials made with construction and demolition waste aggregates. Journal of Cleaner Production. 129, 125-133(2016)

[25] Pasandín, A.R., Pérez, I.: Overview of bituminous mixtures made with recycled concrete aggregates. Construction and Building Materials. 74, 151-161(2015)

[26] Zhu, X., Yuan, Y., Li, L.: Identification of interfacial transition zone in asphalt concrete based on nano-scale metrology techniques. Materials & Design. 129, 91-102(2017)
[27] Matzenmiller, A., Gerlach, S.: Parameter identification of elastic interphase properties in fiber composites. Compos. Part B. 37, 117-126(2005)
[28] Xiao, J.Z., Li, W.G., Sun, Z.H.: Crack propagation in RCA concrete under uniaxial compressive loadin. 109 (4), 451-462(2012)
[29] Mo, L.T., Huurman, M., Wu, S.P., Molenaar, A.A.A.: Bitumen–stone adhesive zone damage model for the meso-mechanical mixture design of ravelling resistant porous asphalt concrete. Int. J. Fatigue. 33 (11), 1490–1503(2011)
[30] Hu, J., Liu, P.F., Huang, Q.B., Qian, Z.D., Luo, S.: Research on interfacial zone failure of asphalt mixture mixed with recycled aggregates. Construction and Building Materials. 319, 126113(2022)
[31] Hu, J., Qian, Z., Wang, D., Oeser, M.: Influence of aggregate particles on mastic and air-voids in asphalt concrete. Constr. Build. Mater. 93, 1–9(2015)
[32] Jiang, J., Ni, F., Dong, Q., Yao, L., Ma, X.: Investigation of the internal structure change of two-layer asphalt mixtures during the wheel tracking test based on 2D image analysis. Constr. Build. Mater. 209, 66–76(2019)
[33] Barbhuiya, S., Caracciolo, B.: Characterisation of Asphalt Concrete Using Nanoindentation. Materials. 10 (7), 823(2017)
[34] Lv, X.B., Fan, W.Y., Wang, J.Q.: Study on adhesion of asphalt using AFM tip modified with mineral particles. Construction and Building Materials. 207, 422-430(2019)
[35] Anna, S., Enric, V.R., Marilda, B.B.: Study of the recycled aggregates nature's influence on the aggregate–cement paste interface and ITZ. Constr. Build. Mater. 68, 677-684(2014)
[36] Xie, Y.T., Corr, D.J., Jin, F.: Experimental study of the interfacial transition zone (ITZ) of model rock-filled concrete (RFC). Cem. Concr. Compos. 55, 23-231(2015)
[37] Hu, J., Huang, Q.B., Lou, N., Luo, S.: Microstructural Characteristics of Interfacial Zone in Asphalt Mixture Considering the Influence of Aggregates Properties. Materials. 13 (13), 2558(2020)
[38] Karki, P., Yuya, P.A., Kim, Y.R., Turner, J.A.: Nanomechanical properties of constituent phases in bituminous mixtures. J. Mater. Civ. Eng. 28 (10), 04016090(2016)
[39] Khorasani, S., Masad, E., Kassem, E.: Nano-mechanical characterization of mastic, aggregate, and interfacial zone in asphalt composites. J. Test. Eval. 41 (6), 924–932(2013)
[40] Lee, G.C., Choi, H.B.: Study on interfacial transition zone properties of recycled aggregate by micro-hardness test. Construction and Building Materials. 40, 455-460(2013)
[41] Tasong, W.A., JLynsdale, C., Cripps, J.C.: Aggregate-cement paste interface: Part I. Influence of aggregate geochemistry. Cement and Concrete Research. 29, 1019-1025(1999)
[42] Li, V.C., Stang, H.: Interface property characterization and strengthening mechan-isms infiber reinforced cement based composites. Adv. Cem. Based Mater. 6, 1-20(1997)
[43] Ministry of Transport of P.R. China, JTG F40-2004, Technical specifications for construction of highway asphalt pavements, China Communications Press, Beijing, 2004.
[44] Miller, M., Bobko, C., Vandamme, M., Ulm, F.J.: Surface roughness criteria for cement paste nanoindentation. Cem. Concr. Res. 38 (4), 467–476 (2008)
[45] Tarefder, R., Faisal, H.: Effects of dwell time and loading rate on the nanoindentation behavior of ssphaltic materials. J. Micromech. Microeng. 3 (2), 17–23(2012)
[46] Tarefder, R., Faisal, H.: Nanoindentation characterization of asphalt concrete aging. J. Nanomech. Micromech. 4 (1), A4013003(2014)
[47] Sanchez-Cotte, E.H., Fuentes, L., Martinez-Arguelles, G., Quintana, H.A.R., Walubita, L.F., Cantero-Durango, J.M.: Influence of recycled concrete aggregates from different sources in hot mix asphalt design. Constr. Build. Mater. 259, 120427(2020)
[48] Hou, YQ., Ji, XP., Zou, L., Liu, S., Su, XL.: Performance of cement-stabilised crushed brick aggregates in asphalt pavement base and subbase applications. Road. Mater.Pavement. 17 (1), 120–135(2016)